# Canopy conductance models: validation for rapidly changing conditions on 1-minute time scale

Van Westreenen, A. *
*Wageningen UR, Meteorology and Air Quality*

Moene, A.F.
*Wageningen UR, Meteorology and Air Quality*

Van Kesteren, B.
*Deutsche Wetter Dienst*

Hartogensis, O.K.
*Wageningen UR, Meteorology and Air Quality*

ABSTRACT

The canopy conductance ($g_c$) is a key-parameter for the energy and carbon balance in almost any kind of atmospheric models, i.e. in their land-surface schemes (LSM) representing land-atmosphere interactions. LSM's rely on a good parameterisation of $g_c$. The most widely used parameterisations are the empirical Jarvis-Stewart (JS) and the plant-physiological A-g$_s$ parameterisations, which relates the assimilation rate ($A_n$) to $g_c$. Nowadays atmospheric models run on increasingly finer resolutions. However, the reliability of the canopy conductance parameterisations remain unknown. This paper aims to validate both parameterisations for short time scales. To gain more insight in the A-g$_s$ parameterisation, its submodels for the internal $CO_2$ concentration ($C_i$) and the net assimilation rate are examined as well. Data from an experiment over growing winter-wheat are used, where turbulent fluxes on 1-min time intervals were obtained with a novel method that combines scintillometry with scalar turbulent measurements. Focus lays on non-stationary conditions caused by rapid changes of the incoming shortwave radiation. The JS- and the A-g$_s$ parameterisation were not able to simulate observed responses of $g_c$ to these conditions. Within the A-g$_s$ parameterisation, $C_i$ was not reproduced realistically. Moreover, our results even suggest that the assumption of $C_i$ being a function of $VPD$ and the $CO_2$ concentration at the leaf surface does not hold for insolation lower than 500 W m$^{-2}$. The variability of $A_n$ was reproduced well by the A-g$_s$ submodel, but its predicted magnitude was too small. We found that this underestimation was crucial in explaining the lack of model performance.
(Document version of May 24, 2014
KEYWORDS: A-gs model, assimilation rate, canopy resistance, internal CO2 concentration, Jarvis-Stewart, stomata

## 1. Introduction

Plants cover more than 70% of Earth's landmass (Huete et al. 2002) and play a crucial role in the energy and carbon balances of the surface and the atmosphere through mechanisms as transpiration and photosynthesis. These mechanisms, on their turn, are regulated by plant stomata. Hence, the surface fluxes of water, $L_vE$, and carbon, $F_{CO2}$, are tightly coupled, because water vapour and $CO_2$ simultaneously pass through the plant stomata (Manzoni et al. 2013). Furthermore, the opening and closing of stomata affect the energy balance by changing the partitioning of the available energy into latent- and sensible heat. Through this effect on the energy balance, the stomata also indirectly influence the boundary layer evolution (Holtslag and Ek 1996; van Heerwaarden et al. 2009; Vilà-Guerau de Arellano et al. 2012).

This aperture is an important variable in land-surface schemes (LSM's) used in numerical weather prediction- and climate models. In those schemes aperture is usually defined as a conductance, which is a measure for the ease with which the exchange of $CO_2$ with the ambient air takes place. The stomatal conductance depends on many environmental conditions, such as temperature, ambient $CO_2$ concentration, water vapour deficit ($VPD$) and radiation (Jacobs 1994). Many stomatal conductance parameteri-

sations have been proposed in literature all dealing in a different way with the dependence on the environmental conditions.

One of the first parameterisations that simulates the stomatal conductance is proposed independently by Jarvis (1976) and Stewart (1988), resulting in the so-called Jarvis-Stewart (JS) stomatal conductance parameterisation. This type of parameterisations is an important part of second generation LSM's (Pitman 2003). In its general form a JS-type stomatal conductance parameterisation is an empirical multiplicative function of a minimum conductance and a number of response functions. This type of stomatal conductance parameterisations is used in numerical weather prediction models like HIRLAM (Unden et al. 2002), COSMO (Doms et al. 2011) and ECMWF (ECMWF 2012).

A third generation LSM uses stomatal conductance parameterisations, more based on plant-physiology, such as the A-$g_s$ parameterisation (Collatz et al. 1991, 1992; Jacobs 1994; Ronda et al. 2001). This parameterisation is partly based on plant physiology and connects the photosynthesis rate and the $CO_2$-concentration difference to the stomatal conductance, $g_{s,c}$. To solve for the stomatal conductance, the A-$g_s$ parameterisation uses submodels for the assimilation rate and the internal $CO_2$-concentration. This parameterisation of $g_{s,c}$ is used in ECMWF for calculating carbon fluxes (ECMWF 2012).

For practical use in models and validating with observations on fields scales the stomatal conductance parameterisations have to scaled up from leaf to canopy level, so that the stomatal conductance parameterisations are also valid on field scales.

The Jarvis-Stewart parameterisation have been empirically developed for field scales and steady-state conditions (i.e. for time scales of $\sim$ 1 hour) (Jarvis 1976; Kim and Verma 1991). The parameterisation is thus calibrated to slowly changing conditions. The A-$g_s$ parameterisation is partly based on laboratory research, e.g. the relation between the stomatal conductance and the photosynthetic rate (Farquhar and Sharkey 1982; Wong 1979). However, also this relationship has been determined for steady-state conditions (Field et al. 1982). This indicates that also the A-$g_s$ parameterisation is (partially) based on results determined under slowly changing conditions. However, nowadays global and mesoscale models run on increasingly finer resolutions forcing an increasingly finer temporal domain. A good representation of rapid changing conditions is even more needed for large eddy simulations (LES), which have spatial scales down to $\Delta x = 1.5m$ and $\Delta z = 1m$ and temporal scales of $\Delta t << 1s$ (Bergot et al. 2014; Maronga et al. 2013). This implies that non-stationary, rapidly changing conditions, such as a decrease of radiation due to clouds, now can be resolved by the models (Vilà-Guerau de Arellano et al. 2014). Therefore it is necessary that the JS- and A-$g_s$ parameterisation perform well on shorter time scales (i.e. $\sim$ minutes).

To validate the two parameterisations turbulent fluxes of the exchange of water vapour and $CO_2$ between the plants and the atmosphere are needed. However, the most widely used method to measure turbulent fluxes, the eddy covariance (EC) method, needs an averaging time of at least 10, but rather 30 minutes (Foken 2008; Van Kesteren et al. 2013a). This is the reason that until now validation of canopy conductance parameterisations at short time scales was not possible. Van Kesteren et al. (2013b) developed a method to measure turbulent fluxes on 1-min time scale, based on a combination of measurements from a fast-response gas analyser and a displaced-beam laser scintillometer. This enables us to validate the Jarvis-Stewart type- and the A-$g_s$ parameterisation at short time scales and under conditions of non-stationarity. Therefore, the aim of this study is to investigate whether the most commonly used canopy conductance parameterisations, the Jarvis-Stewart and A-$g_s$ parameterisations, are valid at field scale for short time scales, especially under conditions of non-stationarity. First, we will validate the canopy conductance as simulated by both parameterisations. Second, we will validate the A-$g_s$ submodels for the internal $CO_2$ concentration and the net assimilation rate to have a closer look at the validity of the A-$g_s$ parameterisation.

The paper is structured as follows. Section 2 describes briefly the JS- and A-$g_s$ canopy conductance parameterisations. Section 3 introduces the research strategy, the experiment and the methodology. Subsequently, the results are presented in section 4. Finally, the discussion and conclusions are presented in section 5 and 6.

## 2. Model description

In the following section we will briefly explain the different models that are used in this study. In section 2a the empirical multiplicative Jarvis-Stewart parameterisation will be explained in more detail, whereas section 2b describes the more plant-physiological A-$g_s$ parameterisation with its submodels for the internal $CO_2$ concentration and net assimilation rate. The parameterisations and submodels will be described in more detail in the appendix. Section 2c describes the soil respiration model that is needed to obtain observations that can be compared with the model.

### *a. Jarvis-Stewart type canopy conductance parameterisation*

There are many different Jarvis-Stewart response functions. We examined the functions as suggested by Jarvis (1976); Kim and Verma (1991); Chen and Dudhia (2001); Irmak and Mutiibwa (2010). The different models show the same behaviour (not shown). Therefore, in this study we will only use the Chen and Dudhia (2001) parameterisation

that is most widely used:

$$g_{c,c} = \frac{g_{c,max} LAI}{1.6} f_1 f_2 f_3 f_4 \quad , \tag{1}$$

$$f_1(S_{in}) = \frac{g_{c,max}/g_{c,min} + f}{1+f}$$

$$\text{where} \quad f = 0.55 \frac{2}{LAI} \frac{S_{in}}{S_{0.5}} \quad , \tag{2}$$

$$f_2(VPD) = \frac{1}{1 + h_s(q_{sat}(T_{leaf}) - q_s)} \quad , \tag{3}$$

$$f_3(T) = 1 - 0.0016 (T_{ref} - T_a)^2 \quad , \tag{4}$$

$$f_4(\theta) = \begin{cases} \theta < \theta_{pwp} & 0 \\ \theta_{pwp} \leq \theta \leq \theta_{fc} & \frac{\theta - \theta_{pwp}}{\theta_{fc} - \theta_{pwp}} \\ \theta > \theta_{fc} & 1 \end{cases} \quad , \tag{5}$$

where, $g_{c,c}$ is the canopy conductance to $CO_2$, $g_{c,max}$ and $g_{c,min}$ are the maximum (=0.025 m $s^{-1}$) and minimum (=0.0002 m $s^{-1}$) canopy conductance, $LAI$ is the leaf area index. The factor 1.6 is to take into account the different diffusivities of water vapour and $CO_2$. $S_{in}$ is the incoming shortwave radiation (W $m^{-2}$), $S_{0.5}$ (=100 W $m^{-2}$) is the amount of radiation where $f_1$ is half its maximum value, $h_s$ (=$3\times10^{-4}$ kg $kg^{-1}$) is a constant showing the sensitivity to the moisture deficit, $q_{sat} - q_s$, (kg $kg^{-1}$), $T_{ref}$ is the reference temperature, which is set to 298 K, $T_a$ is the air temperature (K) and $\theta$ is the volumetric water content ($m^3$ $m^{-3}$), where the subscripts *pwp* and $fc$ denote the permanent wilting point and the field capacity respectively. The parameterisation as suggested by Chen and Dudhia (2001) mostly follows Jacquemin and Noilhan (1990), they explained the parameterisation in more detail.

*b. A-$g_s$ canopy conductance parameterisation*

An approach that is less empirical and more based on physiological and biochemical properties of the plant than the Jarvis-Stewart model is the A-$g_s$ parameterisation, which is extensively described by Jacobs (1994) and Ronda et al. (2001). This parameterisation relates the stomatal conductance to the assimilation rate:

$$g_{s,c} = \frac{A_n}{\rho_{air}(C_s - C_i)} \quad , \tag{6}$$

where, $g_{s,c}$ is the stomatal conductance to $CO_2$ (m $s^{-1}$), $A_n$ is the net assimilation rate (kg $m^{-2}$ $s^{-1}$), $\rho_{air}$ is the air density (kg $m^{-3}$) and $C_s$ and $C_i$ are the ambient (at leaf surface) and internal $CO_2$ concentration (kg $kg^{-1}$) respectively.

The following section describes this parameterisation, where the upscaled parameterisation for the stomatal conductance, the canopy conductance, $g_{c,c}$, is described in the first section. The second and third section describe the submodels for $C_i$ and $A_n$ respectively.

1) CANOPY CONDUCTANCE

A general formulation for the canopy conductance is shown in eq. (6). This formulation of the stomatal conductance is influenced by many environmental factors such as radiation, $VPD$, $C_a$, and temperature, all determined at leaf level (Jacobs 1994). To be at use in atmospheric models the stomatal conductance has to be scaled up from leaf to canopy level. Therefore, the net assimilation is integrated over the canopy, which will be explained in more depth when discussing $A_n$. Integrating over the canopy results in the following simplified equation:

$$g_{c,c} = g_{min,c} + \frac{1}{\rho_{air}} \frac{A_n(T_a, PAR, LAI)}{\Delta_C(C_s, VPD)} \quad . \tag{7}$$

The functions for $A_n$ and $\Delta_C$ represent the two submodels for net assimilation rate and the difference between atmospheric and internal $CO_2$ concentration (kg $kg^{-1}$) respectively. Those submodels will be described in more detail in the following sections. The minimal canopy conductance is set to 0.004 m $s^{-1}$, which represents the conductance when all the stomata are closed. In appendix B the A-$g_s$ parameterisation is explained in more detail.

2) INTERNAL $CO_2$ CONCENTRATION

The canopy conductance depends on $\Delta_C$ (see eq. (7)), which is composed of the ambient $CO_2$ concentration, which is known, and the internal $CO_2$ concentration, i.e. the $CO_2$-concentration in the sub-stomatal cavities, which is described by the submodel. This submodel assumes that $C_i$ is not simply a fraction of $C_s$, but that it also depends on $VPD$ in case of sufficient radiation (Jacobs 1994; Zhang and Nobel 1996):

$$\frac{C_i - \Gamma}{C_s - \Gamma} = f_{max} \left(1 - \frac{VPD}{VPD_0}\right) + f_{min} \frac{VPD}{VPD_0} \quad , \tag{8}$$

where $\Gamma$ is the $CO_2$ compensation point (kg $kg^{-1}$), which is defined as the $CO_2$-concentration where assimilation is equal to respiration (Smith et al. 1976). $VPD_0$ is the value of $VPD$ where the stomata close (Pa), it is a plant physiological propertie. The value of $(C_i - \Gamma)/(C_s - \Gamma)$ ranges from $f_{max}$ to $f_{min}$, where $f_{max}$ (=0.89) is a constant and $f_{min}$ is a function of plant physiological properties (see eq. (B11) for more detail).

3) NET ASSIMILATION RATE

Furthermore the net assimilation rate, $A_n$ (as presented in eq. (7)), is described by another submodel. This submodel describes the amount of $CO_2$ taken up by the plant and used for plant growth. It is defined as the photosynthetic rate, $A_g$, minus the dark respiration rate, $R_d$. To be at use in atmospheric models $A_n$ has to be scaled up from leaf to canopy. Therefore, absorption of sunlight in the

canopy is described as an exponential decay of photosynthetically active radiation ($PAR$), depending on the leaf area index ($LAI$) (Ronda et al. 2001). That means that leaves lower in the canopy receive less $PAR$ and therefore those leaves have less energy for photosynthesis. After integration the simplified equation for $A_n$ becomes:

$$A_n = A_m\left(T_a, C_i\right) \times f\left(PAR, LAI\right) \quad , \tag{9}$$

where, $A_m$ is the assimilation in the mesophyll of the leaf (kg $m^{-2}$ $s^{-1}$) and $f(PAR, LAI)$ contains the radiation- and leaf area dependent part of the $A_n$-model due to integration over the canopy (see eq. (B2) for more detail).

*c. Soil respiration*

When measurements take place on field scale, the measured $CO_2$ flux is the summation of all processes that use and produce $CO_2$, the net ecosystem exchange, $NEE$, which is defined as:

$$NEE = A_n - R_s = A_g - R_d - R_s \quad , \tag{10}$$

where $R_s$ is the soil respiration rate (kg $m^{-2}$ $s^{-1}$). In this study we are only interested in the net assimilation rate. Therefore we need to add the soil respiration to the observed $CO_2$ flux to determine $A_n$. However, the soil respiration was not directly measured. Therefore, the soil respiration model as proposed by Lloyd and Taylor (1994) is used:

$$R_s = R_{s,ref} \times e^{E_0\left(\frac{1}{T_{ref}-T_0} - \frac{1}{T_a - T_0}\right)} \quad , \tag{11}$$

where $R_{s,ref}$ is the soil respiration rate (kg $m^{-2}$ $s^{-1}$) at $T_{ref}$ (283.15K), $T_0$ is 227.13K, which is the temperature where there is no soil respiration anymore. Furthermore, $E_0$ is a temperature sensitivity factor (K).

## 3. Materials and Methods

In the following section we will describe the method that is used to answer the research questions. Section 3a describes the research strategy that is used to validate the parameterisations and submodels. Section 3b will then describe the data that is needed to do this validation. Finally section 3c describes how we obtained the variables that are needed for the validation from the data.

*a. Research strategy*

To validate the canopy conductance parameterisation we will split the validation into two steps. First, the simulated canopy conductances will be compared to observations. This will also be done for $C_i$ and $A_n$ by comparing them with variables that are obtained from the data. As a second step, we will replace the submodels of the A-$g_s$ parameterisation for $C_i$ and $A_n$ by observations of those quantities. Replacing those submodels by observations gives the opportunity to see what the relative importance of the submodels is within the A-$g_s$ canopy conductance parameterisation.

*b. Data*

Data used in this study were collected in the framework of the Transregio32 project (Graf et al. 2010) from May 8, 2009 to June 6, 2009. The measurements were obtained above a well-watered winter-wheat field near Merken (50°, 50′, 53.92″N, 6°, 24′, 1.99″E). In the middle of the field an eddy-covariance system was installed, which measured with a frequency of 20Hz, at 2.4m above the ground. Also a displaced-beam laser scintillometer (Scintec, Rottenburg, Germany) was installed at the same height as the EC system with a path of 120m (Van Kesteren et al. 2013b).

$L_vE$ and $F_{CO2}$ are determined with the structure-parameter method from a combination of scintillometer and high-frequency open-path gas-analyser measurements (Van Kesteren et al. 2013a). The displaced-beam scintillometer provides 1-min path-averaged estimates of the friction velocity and atmospheric stability (Obukhov length) via turbulence induced scattering of its beams along the 120m measurement path (Hartogensis et al. 2002; Thiermann and Grassl 1992). The fast-response gas analyser, on the other hand, provides estimates of the structure parameter of humidity and $CO_2$, $C_q^2$ and $C_{qCO2}^2$, via in situ absorption measurements of infrared radiation (Hartogensis 2006; Tatarskii 1961). Combining these two types of measurements, through the similarity relationships for the structure parameter that are defined in the framework of Monin-Obukhov similarity theory, results in accurate 1-min estimates of $L_vE$ and $F_{CO2}$ (Van Kesteren et al. 2013b).

We are interested in the response of the Jarvis-Stewart and A-$g_s$ models to rapidly changing atmospheric conditions. Three days with such conditions were selected by Van Kesteren et al. (2013b): 2 June, 4 June and 5 June 2009. The variations in atmospheric conditions (fig. 1) are mainly related to varying cloud cover. The clouds on these days resulted in stepwise changes in radiation. Although 2, 4 and 5 June 2009 all had non-stationary conditions, the fluctuations in global radiation on those days were significantly different. The $2^{nd}$ of June was a sunny day, with and without clouds before and after 9:00 UTC respectively. It is an ideal case to see if the model represents the different parts of the day equally well. The $4^{th}$ of June was a cloudy day with some sunny spells and the $5^{th}$ of June shows some sudden decreases in radiation (due to clouds) in the morning.

*c. Data processing*

In the dataset described before there are no direct observations of $g_{c,c}$, $C_i$ and $A_n$. Therefore, the following

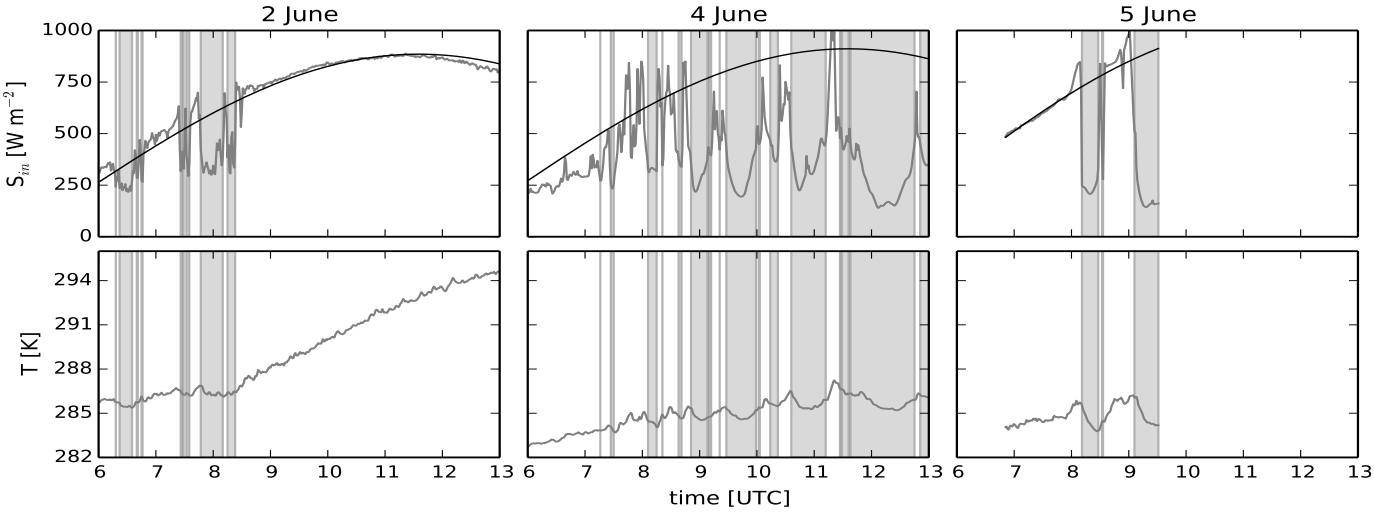


FIG. 1. The most important observed atmospheric variables (grey line), incoming shortwave radiation and temperature (row) for 2, 4 and 5 June 2009 (column). The $VPD$ shows the same pattern as the temperature. The black line indicates the incoming radiation at earth's surface with clear sky transmissivities of 0.68, 0.70 and 0.79 for 2,4 and 5 June respectively, calculated from incoming radiation at the top of the atmosphere (Moene and Van Dam 2014). A reduction of respectively 0.14, 0.32 and 0.30 is defined as being a cloud, this is indicated by the shaded area. This indication will also be used in the following figures.

section describes how the variables that are necessary to validate the parameterisations are obtained from surface fluxes.

1) CANOPY CONDUCTANCE

This study validates the Jarvis-Stewart and A-g$_s$ parameterisations to their representation of the canopy conductance. For validation, we use the canopy conductance as deduced from the observed $L_vE$ (Moene and Van Dam 2014):

$$g_{c,c} = \frac{\left(-\frac{\rho_{air}L_v[q_a - q_{sat}(T_{leaf})]}{L_vE} - \frac{1}{1.6g_{a,c}}\right)^{-1}}{1.6}, \qquad (12)$$

where, $L_vE$ is the latent heat flux (W m$^{-2}$), $L_v$ is the latent heat of vaporization (J kg$^{-1}$), $q_a$ is the specific humidity (kg kg$^{-1}$), $q_{sat}(T_{leaf})$ is the specific humidity inside the stomata (kg kg$^{-1}$), defined as the saturated specific humidity at leaf temperature, $T_{leaf}$ (K). $T_{leaf}$ is approximated with the surface temperature, $T_{sfc}$. Furthermore, $g_{a,w}$ is the aerodynamic conductance to water vapour (m s$^{-1}$), which is determined using the conductance expression for sensible heat (Moene and Van Dam 2014). The first term of the right-hand side behind parentheses of eq. (12) can be considered as the total conductance. Occasionally, it happened that the total and aerodynamic conductance were similar, pushing the canopy conductance towards infinity; these data were omitted as mathematical artefacts.

Although there is an expression to deduce the canopy conductance from, we need to be aware that the variables in eq. (12) are evaluated at measuring height. However, Van Kesteren et al. (2013b) showed that there is a time lag between observed and surface fluxes, where we want to know $g_{c,c}$, due to storage below the measurement device. Therefore, we will follow Van Kesteren et al. (2013b) by taking into account the storage below the measurement device to ensure that the surface fluxes are equal to the fluxes at observation height.

2) INTERNAL $CO_2$ CONCENTRATION

A further validation of the A-g$_s$ model can be done by looking at the submodel for the internal $CO_2$ concentration. In this submodel it is assumed that $C_i$ depends on $C_s$ and $VPD$, we will validate this assumption. However, as $C_i$ cannot be measured directly, $C_i$ will be deduced from the conductance expression for the $CO_2$ flux:

$$F_{CO2} = -\frac{C_s - C_i}{\frac{1}{g_{a,c}} + \frac{1}{g_{c,c}}} + R_s \quad , \qquad (13)$$

where $F_{CO2}$ is the $CO_2$ flux as measured (kg m$^{-1}$ s$^{-1}$), $C_s$ is the $CO_2$ concentration at leaf level (kg kg$^{-1}$), $g_{a,c}$ is the aerodynamic conductance to $CO_2$ (m s$^{-1}$). The soil respiration needs to be taken into account since the flux observations include both the $CO_2$ uptake by plants and the $CO_2$ release by the soil.

It can be seen from eq. (8) that the modelled internal

$CO_2$ concentration also depends on $C_s$, which is affected by varying environmental conditions. To prevent that fluctuations in modelled $C_i$ are only caused by fluctuations in $C_s$, this submodel will be validated according to the difference between $C_i$ and $C_s$.

The soil respiration model (eq. (11)) is calibrated during night-time conditions when there is no incoming shortwave radiation and thus no photosynthesis, hence the observed $CO_2$ flux equals the soil respiration rate. For this analysis, data are neglected when the friction velocity, $u^*$, is lower than 0.1 m $s^{-1}$ (Jacobs et al. 2007), because during calm nights turbulence is suppressed and fluxes are not reliable. Linear regression is then applied to the linearized version of eq. (11). From the intercept $R_{s,ref}$ is determined and the temperature sensitivity, $E_0$, is found as the slope of the regression line.

Once the parameters $R_{s,ref}$ and $E_0$ have been determined, the soil respiration is extrapolated to day-time conditions using the temperature dependency (Janssens et al. 2001; Rambal et al. 2003; Reichstein et al. 2005).

3) Net assimilation rate

Also the second submodel of the A-$g_s$ model allows for a closer validation of the model. However, this submodel predicts the net assimilation rate, $A_n$, while the $CO_2$ flux at measuring height is equal to the $NEE$. Therefore, the soil respiration is added to $NEE$ in order to obtain $A_n$ from $NEE$(eq. (10)).

*d. Error Measure*

Model performance is evaluated with a set of regression-based and error-based statistical parameters. Here we use parameters mostly used by Op de Beeck et al. (2010), who also validated stomatal conductance models. The regression-based parameters that are used to validate the models are the slope, intercept and Pearson's correlation coefficient ($r$), which are determined from a linear regression between the simulation and the observations. Furthermore, the error-based statistical parameters include the mean bias ($MB$), the root mean squared error ($RMSE$) and the model efficiency ($ME$) (Nash and Sutcliffe 1970).

For this study we are mainly interested in the response of the model to rapidly changing conditions, not in the overall bias. Therefore, a bias-corrected $RMSE$ ($BCRMSE$) and a bias-corrected model efficiency are introduced. A more elaborate explanation of the statistical parameters can be found in appendix A.

Besides the model validation with the above described statistical parameters the model will also be validated on how well it predicts the right values at the right time. This is checked by determining an optimal time lag, $lag$, based on the lag for which the cross correlation between observations and model gives the highest correlation. The smaller the time lag, the better the model performance.

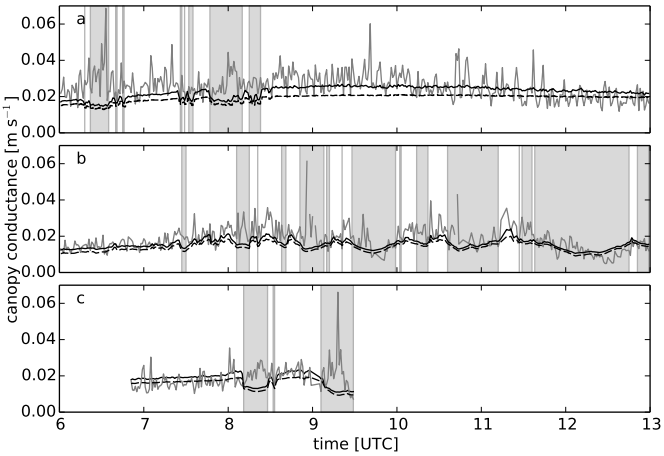


FIG. 2. observed (grey line) and modelled canopy conductance as simulated by the Jarvis-Stewart parameterisation (dashed black line) and the A-$g_s$ parameterisation (solid black line) for (a) 2 June, (b) 4 June and (c) 5 June 2009. Shaded areas indicate cloud occurance.

## 4. Results

In this section we will describe the results of the validation. Section 4a gives the validation results of the Jarvis-Stewart and A-$g_s$ canopy conductance parameterisations. Furthermore, in section 4b and 4c the validation of the submodels for $C_i$ and $A_n$ will be described.

*a. Canopy conductance*

Eq. 1 showed that the modelled canopy conductance respond to radiation, $T$, $VPD$ and $\theta$. Since there are well-watered conditions there will be no soil moisture stress that has an effect on the canopy conductance, so the soil moisture response can be neglected. Moreover, the modelled canopy conductance linearly respond to the incoming radiation. Therefore, the conductance should show the same variation as the radiation. Furthermore, the temperature and $VPD$ response are rather slow compared to radiation and has no large influence on the rapid fluctuations of $g_{c,c}$. Fig. 2 shows the modelled and observed canopy conductance for the three different cases as introduced in section 3b. It can be seen that the difference between the JS- and A-$g_s$ parameterisation is small, albeit that the response to varying radiation of the A-$g_s$ parameterisation is slightly stronger than the response of the JS-parameterisation. This is supported by a slightly higher $r$ for the A-$g_s$ parameterisation (table 2). Because the difference between JS- and A-$g_s$ parameterisations is small, we will treat them simultaneously, except when indicated otherwise, in the following part of this section. The mod-

TABLE 1. Values of the different statistical parameters for the canopy conductance as simulated by the Jarvis-Stewart canopy conductance parameterisation. Statistical indices are calculated for the period before and after 9:00 UTC. Note that average and the optimal time lag are calculated for the whole day.

| | June 2 | | June 4 | | June 5 | |
|---|---|---|---|---|---|---|
| quantity | before 9 | after 9 | before 9 | after 9 | before 9 | after 9 |
| Intercept [m $s^{-1}$] | 0.017 | 0.020 | 0.011 | 0.010 | 0.017 | 0.012 |
| Slope [-] | 0.007 | 0.035 | 0.186 | 0.175 | -0.018 | -0.032 |
| Pearson's r [-] | 0.025 | 0.602 | 0.485 | 0.600 | -0.041 | -0.149 |
| MB [m $s^{-1}$] | 0.010 | 0.004 | 0.005 | 0.003 | 0.002 | 0.010 |
| RMSE [m $s^{-1}$] | 0.012 | 0.008 | 0.008 | 0.006 | 0.006 | 0.016 |
| BCRMSE [m $s^{-1}$] | 0.002 | 0.004 | 0.002 | 0.003 | 0.004 | 0.006 |
| ME [-] | -0.072 | 0.066 | 0.220 | 0.309 | -0.238 | -0.109 |
| average $g_{c,c}$ [m $s^{-1}$] | 0.019 | | 0.014 | | 0.016 | |
| optimal time lag [min] | 0 | | 10 | | 15 | |

elled absolute values compare well with the observations, whereas the response to rapidly changing conditions do not. Together with the noisy behaviour of the data this results in relatively low correlations for the whole day ranging from -0.141, for June 5, to 0.539 for June 4.

Upon a closer look at the cloud events (shaded areas in fig. 2) we see that for the events after 9:00 UTC the modelled and observed values correlate well. On the other hand cloud events before 9:00 UTC show a counter-intuitive behaviour between observed and modelled $g_{c,c}$. The difference between before and after 9:00 UTC can also be seen in table 1 and 2. The correlation coefficient, $r$, and also $ME$ is higher for the period after 9:00 UTC than the period before 9:00 UTC. The slope and $r$ are however close to 0 for the first part of the day, indicating a poor correlation.

For the period after 9:00 UTC the correlation coefficients range from -0.150 to 0.644, where the negative $r$ is found for June 5, which has relatively few data points after 9:00 UTC. The range of $r$ found for June 2 and 4 is of the same order of magnitude as 0.557-0.768 found by Op de Beeck et al. (2010), although they studied the overall performance of the JS- and A-$g_s$ parameterisation on daily time scales. This makes it difficult to compare with the results of this study, because we calculate $r$ only for separate days, whereas most studies concerning canopy conductance parameterisations study the performance on daily time scales for a combination of multiple days (Op de Beeck et al. 2010; Irmak and Mutiibwa 2010; Jacobs 1994).

The different behaviour between the first and second part of the morning shows that there may be mechanisms, that are not implemented in the model or not well understood. This will be discussed in section 5.

Besides the absolute values of the responses, the canopy conductance parameterisations have to predict the responses to rapidly changing conditions at the right time. Fig. 2 shows especially for June 4 that there is a time lag between the observed and modelled response to a step-change in incoming radiation. The found optimal time lags (table 1 and 2) differ substantially between the different days. This difference may have to do with different radiation regimes, because the reaction time of stomata depend on the amplitude of fluctuations in radiation and on actual opening and closing rates (Woods and Turner 1971).

*b. Internal $CO_2$ concentration*

Another way to validate the A-$g_s$ model is through its submodels. One of those submodels is the submodel for the internal $CO_2$ concentration, which in this study will be treated as the difference between $C_s$ and $C_i$. However, before this parametrization can be examined the soil respiration needs to be taken into account (see eq. (13)). The model presented in eq. (11) is first calibrated with night-time data. The calibration resulted in a temperature sensitivity, $E_0$, of 176.7K. This is within the range of 101K to 263K as found by Reichstein et al. (2005). The reference soil respiration, $R_{s,ref}$, is found to be $2.29\times10^{-7}$ kg $m^{-2}$ $s^{-1}$. It turned out that the correlation between modelled and observed soil respiration was higher when the model was driven by the air temperature, $T_a$, in contrast to the radiation temperature, $T_s$. Therefore, this study uses $T_a$ to determine the soil respiration.

As widely accepted $C_i - \Gamma/C_s - \Gamma$ is only a function of $VPD$. Therefore, $\Delta_C$ should not show large fluctuations when the radiation drops, but only follows the $VPD$. This behaviour is indeed simulated by the submodel (fig. 3). Furthermore, modelled $\Delta_C$ is of the same order of magnitude as the observed difference. The submodel is able to reproduce the course of the day, which is also supported by the low bias. However, there are large fluctuations of observed $\Delta_C$ which are not shown by the submodel, when

TABLE 2. Values of the different statistical parameters for the canopy conductance as simulated by the A-g$_s$ canopy conductance parameterisation. Statistical indices are calculated for the period before and after 9:00 UTC. Note that average and the optimal time lag are calculated for the whole day.

| | June 2 | | June 4 | | June 5 | |
|---|---|---|---|---|---|---|
| quantity | before 9 | after 9 | before 9 | after 9 | before 9 | after 9 |
| Intercept [m s$^{-1}$] | 0.020 | 0.021 | 0.012 | 0.011 | 0.019 | 0.014 |
| Slope [-] | 0.026 | 0.121 | 0.186 | 0.257 | 0.007 | -0.032 |
| Pearson's r [-] | 0.059 | 0.644 | 0.477 | 0.620 | 0.012 | -0.150 |
| MB [m s$^{-1}$] | 0.007 | 0.000 | 0.003 | 0.002 | -0.001 | 0.008 |
| RMSE [m s$^{-1}$] | 0.010 | 0.007 | 0.007 | 0.006 | 0.005 | 0.015 |
| BCRMSE [m s$^{-1}$] | 0.003 | 0.006 | 0.003 | 0.004 | 0.006 | 0.007 |
| ME [-] | -0.139 | 0.207 | 0.220 | 0.342 | -0.305 | -0.111 |
| average $g_{c,c}$ [m s$^{-1}$] | 0.023 | | 0.016 | | 0.018 | |
| optimal time lag [min] | 0 | | 10 | | 16 | |

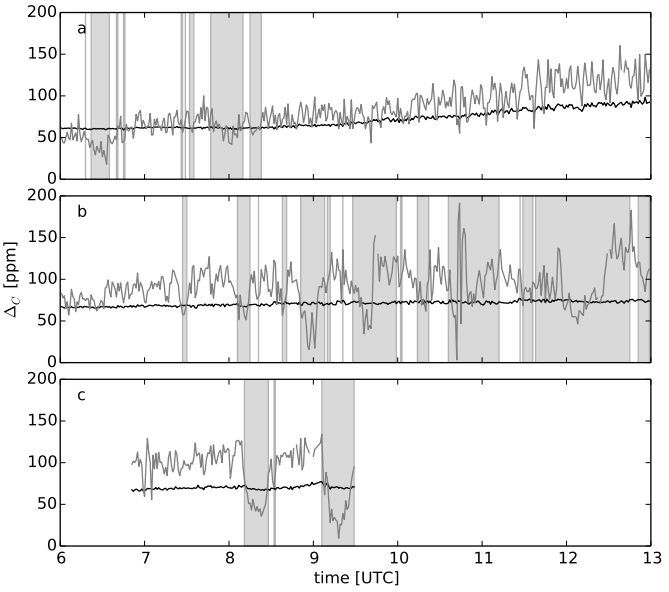


FIG. 3. observed (grey line) and modelled (black line) difference between leaf surface and internal $CO_2$ concentration as simulated by the $C_i$ submodel for (a) 2 June, (b) 4 June and (c) 5 June 2009.

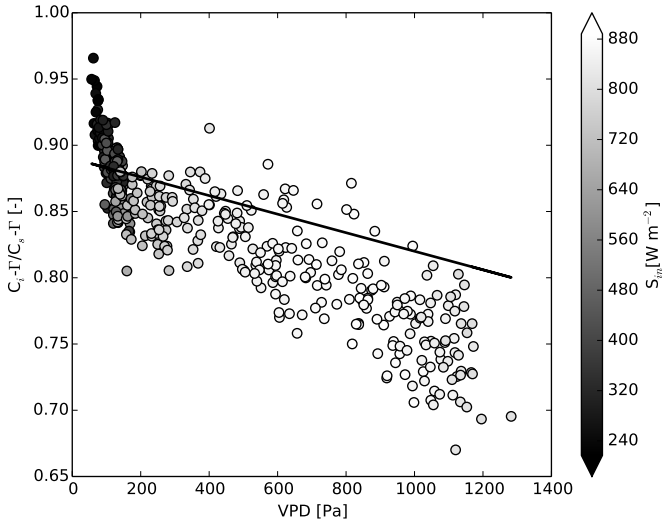


FIG. 4. scatterplot of observed (circles) and modelled (black line) $C_i - \Gamma / C_a - \Gamma$ against VPD of 2 June 2009. Fill-colour of the circles shows the amount of incoming shortwave radiation.

the radiation drops. The decorrelation is also found in table 3, where high intercepts with low slopes and low $r$'s indicate no correlation. The large fluctuations are mainly due to large fluctuations of $C_i$, which may be caused by a difference in the reaction time of $g_{c,c}$ and $A_n$. Vico et al. (2011) showed that $g_{c,c}$ needs some time to adjust to new conditions, whereas $A_n$ reacts instantaneous to changing radiation (Op de Beeck et al. 2010).

The submodel is only valid when there is sufficient light, but this is poorly described in literature. Therefore, fig. 4 shows $C_i - \Gamma / C_s - \Gamma$ against $VPD$ and incoming radiation for June2, 2009. It can be seen that there is a good correlation for higher $VPD$, albeit that the model is slightly higher than observed. Furthermore, the insolation was always larger than 220 W m$^{-2}$. However, for radiation levels lower than 500 W m$^{-2}$ the modelled and observed fraction do not correlate anymore. This is an indication that the submodel for $C_i$ needs at least 500 W m$^{-2}$ to be valid. This signal is less clear for the other days (not shown).

TABLE 3. Values of the different statistical parameters for the difference between leaf surface and internal $CO_2$ concentration as simulated by the submodel for the internal $CO_2$ concentration.

| | *2 June* | *4 June* | *5 June* |
|---|---|---|---|
| Intercept [ppm] | 41.4 | 68.0 | 67.7 |
| Slope [-] | 0.34 | 0.032 | 0.023 |
| Pearson's r [-] | 0.867 | 0.275 | 0.316 |
| MB [ppm] | 11.8 | 19.6 | 20.2 |
| RMSE [ppm] | 21.0 | 30.6 | 34.1 |
| BCRMSE [ppm] | 9.23 | 11.0 | 13.9 |
| ME [-] | 0.547 | 0.050 | 0.040 |
| Average $\Delta_C$ [ppm] | 71.4 | 70.8 | 69.8 |

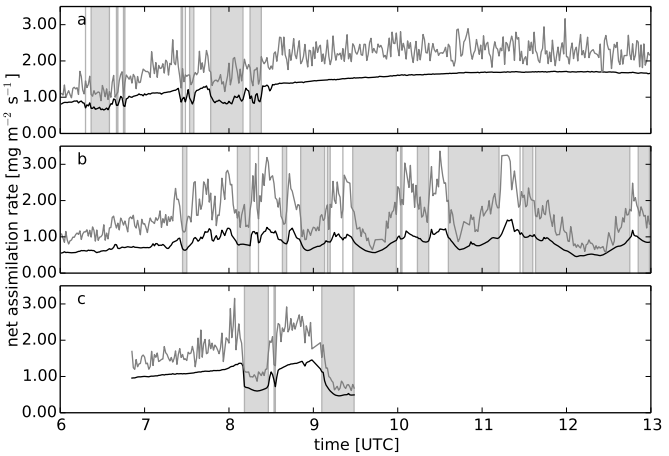


FIG. 5. observed (grey line) and modelled (black line) net assimilation rate for (a) 2 June, (b) 4 June and (c) 5 June 2009.

*c. Net assimilation rate*

The other submodel of the A-g$_s$ canopy conductance parameterisation that can be validated to its response to rapidly changing conditions is the submodel for the net assimilation rate.

The net assimilation rate is proportional to $PAR$. Therefore, the net assimilation rate should follow the radiation and should thus decrease during cloud events. Furthermore, the net assimilation rate reacts faster than $g_{c,c}$ to environmental changes. Therefore, the expectation is that the optimal time lag found in this study is lower than for $g_{c,c}$.

Fig. 5 shows that the submodel underestimates the net assimilation rate, but there is a high correlation between the observations and the model results. Even the responses to changing radiation are well represented by the submodel, which is also supported by the high correlation coefficients (table 4). Correlation coefficients needs to be higher than 0.6 in order to observe a trend in the data (Ott and Longnecker 2010). With correlation coefficients of 0.828 upto 0.903 it is thus possible to see that trend, even for rapidly changing conditions.

Upon a closer look, the response of $A_n$ is slightly underestimated. The underestimation of $A_n$ is supported by the slope of the regression line, which is lower than unity. Furthermore, it is striking that the submodel for $A_n$ also models the responses before 9:00 UTC well. Especially, because the canopy conductance is proportional to the assimilation rate, but $g_{c,c}$ shows an opposite response to decreasing radiation.

The timing of the submodel for $A_n$ is perfect. No time lag is observed, indicating that for the submodel simulates the response to decreasing radiation at the right time.

*d. Relative importance of $C_i$ vs. $A_n$*

To investigate which submodel of the A-g$_s$ canopy conductance parameterisation is most important in modelling $g_{c,c}$, we replace the submodels for $C_i$ and $A_n$ by observations of those quantities.

Replacing the submodel for $C_i$ by observations of $C_i$ does not have a large effect on the performance of the submodel for $A_n$ and the parameterisation for $g_{c,c}$. On average 1% to 7% lower values for $A_n$ are found. $g_{c,c}$ only changes 5% when observations of $C_i$ are implemented in the model. Furthermore, correlations between modelled and observed $A_n$ and $g_{c,c}$ do not change significantly.

On the other hand, replacing the modelled $A_n$ with observations results in higher correlations for $g_{c,c}$. Especially the slopes of the regression lines change considerably. For June 4, which is the day where the change is most clear, for the period before 9:00 UTC the slope increases to 0.489 and for the period after 9:00 UTC the slope becomes 0.637.

TABLE 4. Values of the different statistical parameters for the net assimilation rate as simulated by the A-g$_s$ submodel for $A_n$.

| | *2 June* | *4 June* | *5 June* |
|---|---|---|---|
| Intercept [mg m$^{-2}$ s$^{-1}$] | 0.149 | 0.325 | 0.285 |
| Slope [-] | 0.611 | 0.317 | 0.449 |
| Pearson's r [-] | 0.829 | 0.903 | 0.881 |
| MB [mg m$^{-2}$ s$^{-1}$] | 0.637 | 0.783 | 0.601 |
| RMSE [mg m$^{-2}$ s$^{-1}$] | 0.686 | 0.882 | 0.684 |
| BCRMSE [mg m$^{-2}$ s$^{-1}$] | 0.049 | 0.099 | 0.084 |
| ME [-] | 0.678 | 0.511 | 0.638 |
| Average $A_n$ [mg m$^{-2}$ s$^{-1}$] | 1.384 | 0.838 | 1.005 |
| optimal time lag [min] | 0 | 0 | 0 |

The increase of the slopes indicate that especially the response to changes in radiation is better represented by the A-$g_s$ parameterisation when observations of $A_n$ are implemented in the A-$g_s$.

The foregoing indicates that the $A_n$ submodel is mainly responsible for the response to changing atmospheric conditions for the A-$g_s$ canopy conductance parameterisation. Furthermore, another variable than $C_i$ is responsible for the performance of the $A_n$ submodel, because replacing modelled $C_i$ by observations does not increase the performance of the submodel.

## 5. Discussion

The following section presents the discussion for the canopy conductance, internal $CO_2$ concentration and the net assimilation rate respectively.

### *a. Canopy conductance*

In this study two different and widely used canopy conductance parameterisations are validated. This validation is first done for the canopy conductance. To determine the canopy conductance we needed surface fluxes, because $g_{c,c}$ is not directly measured. In this study surface fluxes were determined by shifting the observed fluxes 2 minutes in time to account for storage in the air below observation level (Van Kesteren et al. 2013b). Storage in the air space below observation level will lead to flux divergence, resulting in a change of the $CO_2$ concentration. Storage may thus be indicated when a change of the observed $CO_2$ flux is preceded by a $CO_2$ concentration change. Examination of this relation indeed shows a dependency between the change of the flux and the change of the concentration and thus storage, albeit that the correlation is of the order of 0.4. Using this relation a time lag of 1-2 minutes due to storage of $CO_2$ is found. We may thus conclude that relating the observed fluxes at 2.4m to the surface fluxes by shifting the measured fluxes 2 minutes in time is a good approximation.

Based on these estimated surface fluxes the 'observed' canopy conductance was determined. A remarkable result was that before 9:00 UTC the canopy conductance peaked during cloud events, whereas the expectation was that during cloud events the canopy conductance should decrease. A first explanation can be that during these events there is more diffuse radiation, which can further penetrate into the canopy (Urban et al. 2012). Therefore more stomata receive sufficient light and thus more stomata will open, which increases the overall canopy conductance (Dengel and Grace 2010). However, this would also lead to an increased assimilation rate (Dengel and Grace 2010), which is not found in this study.

A second explanation may be that under cloudy conditions there is a relative increase in blue light within the canopy compared to clear sky conditions (Dengel and Grace 2010). Because blue light evokes stomatal opening (Hogewoning et al. 2010), cloudy conditions could lead to a higher canopy conductance.

These explanations suggest that cloudy events always result in higher canopy conductances. However, fig. 2 shows that after 9:00 UTC the canopy conductance follows the radiation instead. This may imply that there are also other processes that play a role in determining the canopy conductance, such as plant hormones (Raghavendra et al. 2010) and endogenous rhythms. Endogenous rhythms, with a cycle of 24 hours, are involved in controlling the responsiveness (i.e. rapidity and magnitude of the response) of the stomata to changing environmental conditions (Gorton et al. 1993). From the data as presented in this study it is not possible to decide on the mechanism that is responsible for the inversely proportional relation between radiation and $g_{c,c}$ before 9:00 UTC.

Both the Jarvis-Stewart and A-$g_s$ canopy conductance parameterisations for $g_{c,c}$ were equally successful in simulating the course of the day, but equally unsuccessful in simulating $g_{c,c}$ on 1 minute time scale. That means that both models can be used in land-surface models, but great care has to be taken when time sales become smaller and conditions are not stationary. Also the distinction between before and after 9:00 UTC is something that has to be taken into account.

### *b. Internal $CO_2$-concentration*

As a part of the validation of the A-$g_s$ model also the submodel for $C_i$ is validated. The validation is done with data determined on field scales and at measuring height. With data measured at measuring height (i.e. 2.4m) different locations in the canopy, all with their own properties and processes, have an effect on the observations. Within the canopy temperature changes with height (Waggoner and Reifsnyder 1968; Graser et al. 1987), this is also the case for humidity (Waggoner and Reifsnyder 1968). In this study the field scale measurements are scaled down to canopy level without taking into account this vertical variation of environmental factors. However, it is not known what the effect of different profiles on the derived internal $CO_2$ concentration is.

Furthermore, the observed $\Delta_C$ shows a big dependence on radiation, whereas the model did not. Fig. 4 confirms this and shows that $C_i$ is not simply a function of $C_a$ and $VPD$ for 1-min time scales. This is also mentioned by Jacobs (1994), although they found the effect of other factors to be rather small. Mott (1990) indicates that changes in photosynthetic rate also mediate plant responses to $C_i$. Nevertheless, the dependence of $\Delta_C$ on $VPD$ remains widely accepted for slowly changing environmental conditions (Zhang and Nobel 1996; Jacobs 1994; Ronda et al. 2001).

*c. Net assimilation rate*

Finally also the submodel for net assimilation rate was validated. The submodel for $A_n$ underestimated the absolute values, but especially the response of $A_n$ to varying radiation. The underestimation of $A_n$ can be due to incorrect parameterisation of processes that depend on solar angle and different canopy characteristics (i.e. row spacing and plant population density) such as extinction within the canopy (Evers et al. 2009) or light use efficiency (Brodrick et al. 2013).

## 6. Conclusion

This study discusses the validation of two different canopy conductance parameterisations, the Jarvis-Stewart and A-$g_s$ parameterisations, on short time scales of non-stationary conditions. Furthermore, the submodels for the internal $CO_2$ concentration and the net assimilation rate are validated for these conditions. The validation is based on data collected above growing winter-wheat near Merken, Germany, in the framework of Transregio32 in 2009.

The canopy conductance is not well represented by both the JS- and the A-$g_s$ parameterisations; especially regarding the response to rapidly changing radiation. The responses were too weak and before 9:00 UTC the direction of the change was wrong.

Within the A-$g_s$ model, the submodel for the internal $CO_2$ concentration was not able to simulate the responses to rapidly varying conditions. Our results suggest that the assumption of $C_i$ being only a function of $VPD$ and $C_a$ does not hold for rapidly changing conditions.

On the other hand, the submodel for the net assimilation rate performed well. However, the submodel underestimated the absolute values, but the amplitude of the modelled response was too small compared to observations. We found that this underestimation was crucial in explaining the lack of model performance.

Although various studies among others showed that the Jarvis-Stewart (Jarvis 1976; Stewart 1988; Kim and Verma 1991; Op de Beeck et al. 2010) and the A-$g_s$ parameterisation (Jacobs 1994; Ronda et al. 2001; Op de Beeck et al. 2010) performed well under slowly changing conditions, this study shows that for rapidly changing atmospheric conditions the model has difficulties in accurately representing the canopy conductance, internal $CO_2$ concentration and net assimilation rate.

It appeared that the response of the canopy conductance parameterisation showed a wrong direction before 9:00 UTC. What is the mechanism behind this response? What does 9:00 UTC mean for the plant and does it differ between day of the year? Furthermore, our results suggest that the internal $CO_2$ concentration, $C_i$, is not only a function of the ambient $CO_2$ concentration and the vapour pressure deficit. Which processes are also influencing $C_i$? How is the difference in response time between the canopy conductance and the net assimilation rate influencing $C_i$? The relative importance of the net assimilation rate, $A_n$, for simulating the canopy conductance indicated that it is most important that $A_n$ is well represented. How can this submodel be improved and which processes are important? Is the assumption of exponential decay of radiation sufficient to scale up the assimilation rate from leaf to canopy level?

*Acknowledgments.*

The authors thank those people that were involved in the Transregio32 2009 project. Furthermore, we thank internal and informal reviewers for their supportive comments to improve this paper.

## APPENDIX A

### Error Measure

First of all a linear regression is performed between the observed, $O$, and simulated, $S$, values. From this the regression-based slope, intercept and pearson's correlation coefficient are calculated, where the correlation coefficient, $r$, is computed as follows:

$$r = \frac{\sum_{i=1}^{n} \left(O_i - \bar{O}\right)\left(S_i - \bar{S}\right)}{\sqrt{\sum_{i=1}^{n} \left(O_i - \bar{O}\right)^2} \sqrt{\sum_{i=1}^{n} \left(S_i - \bar{S}\right)^2}} \quad , \tag{A1}$$

where, $i$ denotes the samples, $n$ is the length of the time serie and the overbar indicates the mean of the observed and simulated values.

Furthermore, some error-based statistical parameters are worked out. The mean bias ($MB$) shows the mean difference between the observed and simulated values, and is given by:

$$MB = \frac{1}{n} \sum_{i=1}^{n} \left(O_i - S_i\right) \quad . \tag{A2}$$

The root mean squared error ($RMSE$) is the square root of the mean squared difference between the modelled and measured values and is given by:

$$RMSE = \sqrt{\frac{1}{n} \sum_{i=1}^{n} \left(O_i - S_i\right)^2} \quad . \tag{A3}$$

The $RMSE$ can also be calculated from $MB$ and the variance of the error, $\sigma^2_{S-O}$, which is the square of the standard deviation of the error, $\sigma_{S-O}$, using:

$$BCRMSE = RMSE - MB \quad . \tag{A4}$$

The variance of the error is referred to as the bias-corrected $RMSE$ ($BCRMSE$), because it removes the overall bias (Gotway et al. 2012).

The last error-based parameter that is introduced is the Model Efficiency ($ME$) as proposed by Nash and Sutcliffe (1970), which is given by:

$$ME = 1 - \frac{\sum_{i=1}^{n} (O_i - S_i)^2}{\sum_{i=1}^{n} (O_i - \bar{O})^2} \quad . \tag{A5}$$

Values of $ME$ range from $-\infty$ to 1. A value of 1 means a perfect agreement between the model and the observations. Values between 0 and 1 are generally viewed as acceptable values. Values lower than 0 indicate that the mean observed value is a better predictor than the simulated value, which makes a model unacceptable (Moriasi et al. 2007).

However, because we are mainly interested in the response of the model to rapidly changing conditions, the definition of eq. (A5) is not very useful, because it does not correct for the bias. Because the numerator of $ME$ is equal to the mean square error ($MSE$) it can be replaced by a bias-corrected $MSE$ (BCMSE). According to eq. (A4) $BCMSE = BCRMSE^2$. Eq. (A5) then becomes:

$$ME = 1 - \frac{BCMSE}{\sum_{i=1}^{n} (O_i - \bar{O})^2} \quad . \tag{A6}$$

## APPENDIX B

### A-g$_s$ parameterisation formulation

In this appendix the plant-physiological based A-g$_s$ parameterisation as described by Jacobs (1994); Collatz et al. (1991, 1992); Ronda et al. (2001) is presented.

The A-g$_s$ parameterisation is presented in parallel with eq. (7), which is presented again for clarity:

$$g_{c,c} = g_{min,c} + \frac{1}{\rho_{air}} \frac{A_n (T, PAR, LAI)}{\Delta_C (C_s, VPD)} \quad , \tag{B1}$$

This parameterisation is build up from different submodels for the net assimilation rate, $A_n$, and the difference between leaf surface and intercellular $CO_2$ concentration, $\Delta_C$. The net assimilation rate is integrated over the canopy (i.e. $LAI$) and becomes:

$$A_n = A_m \left\{ LAI - \frac{1}{K_x} \left[ E_1 \left( \frac{\alpha K_x PAR}{A_m + R_d} e^{-K_x LAI} \right) - E_1 \left( \frac{\alpha K_x PAR}{A_m + R_d} \right) \right] \right\} , \tag{B2}$$

where $R_d$ is the dark respiration rate (kg m$^{-2}$ s$^{-1}$), $\alpha$ is the light use efficiency (kg J$^{-1}$), $K_x$ is the extinction coefficient (-) (table 5) and $E_1(x)$ is the exponential integral of the first order with argument $x$. This equation is replacing $A_n(T, PAR, LAI)$ in eq. (B1). Furthermore, the canopy conductance as calculated with eq. (B1) also depends on $\Delta_C(C_s, VPD)$. This variable is derived from the ratio of the internal $CO_2$ concentration to leaf surface $CO_2$ concentration:

$$\frac{C_i - \Gamma}{C_s - \Gamma} = f_{max} \left( 1 - \frac{VPD}{VPD_0} \right) + f_{min} \frac{VPD}{VPD_0} \quad , \tag{B3}$$

where, $\Gamma$ is the compensation point (kg kg$^{-1}$). After implementation of this submodel into eq. (B1) the formulation for the canopy conductance becomes:

$$g_{c,c} = g_{min,c} LAI + \frac{1}{\rho_{air}} \frac{\frac{1}{1-f_{max}} (A_m + R_d)}{(C_s - \Gamma) \left( 1 + \frac{f_{max} - f_{min}}{1 - f_{max}} \frac{VPD}{VPD_0} \right)} \times \left\{ LAI - \frac{1}{K_x} \left[ E_1 \left( \frac{\alpha K_x PAR}{A_m + R_d} e^{-K_x LAI} \right) - E_1 \left( \frac{\alpha K_x PAR}{A_m + R_d} \right) \right] \right\} . \tag{B4}$$

Important variables in eq. (B4) are $A_m$ and $R_d$, which are calculated as follows:

$$A_m = A_{m,max} \left( 1 - e^{-\frac{g_m (C_i - \Gamma)}{A_{m,max}}} \right) \quad , \tag{B5}$$

$$R_d = 0.11 A_m \quad , \tag{B6}$$

$$\alpha = \alpha_0 \frac{C_s - \Gamma}{C_s + 2\Gamma} \quad , \tag{B7}$$

where $A_{m,max}$ is the maximum primary productivity (kg m$^{-2}$ s$^{-1}$), $g_m$ is the mesophyll conductance (m s$^{-1}$) and $\alpha_0$ is the initial light use efficiency (i.e. under low light conditions) (kg J$^{-1}$)(table 5). For determining the primary productivity, $A_m$, and thus the dark respiration rate, $R_d$, the temperature is an important variable:

$$g_m = \frac{g_{m,ref} Q_{10}^{(T_l - 298)/10}}{\left[ 1 + e^{0.3(T_1 - T_l)} \right] \left[ 1 + e^{0.3(T_l - T_2)} \right]} \quad , \tag{B8}$$

$$A_{m,max} = \frac{A_{m,max,ref} Q_{10}^{(T_l - 298)/10}}{\left[ 1 + e^{0.3(T_1 - T_l)} \right] \left[ 1 + e^{0.3(T_l - T_2)} \right]} \quad , \tag{B9}$$

$$\Gamma = \Gamma_{ref} Q_{10}^{(T_l - 298)/10} \quad , \tag{B10}$$

where $g_{m,ref}$, $A_{m,max,ref}$ and $\Gamma_{ref}$ are $g_m$, $A_{m,max}$ and $\Gamma$ respectively at reference temperature of 298K, $Q_{10}$ is the rate of change of a chemical reaction as a consequence of increasing the temperature by 10K and $T_l$ is the leaf temperature. The ratio of $(C_i - \Gamma)/(C_s - \Gamma))$ varies between $f_{min}$ and $f_{max}$. Here $f_{max}$ (-) is a constant and $f_{min}$ (-) is a function of $g_{min,c}$ and $g_m$:

$$f_{min} = \frac{\sqrt{(g_{min,c} - 0.11 g_m)^2 + 4 g_{min,c} g_m}}{2 g_m} - \frac{g_{min,c} - 0.11 g_m}{2 g_m} . \tag{B11}$$

TABLE 5. Parameter values for the biochemical module (i.e. the module that represents biochemical processes in the plant) in the A-$g_s$ parameterisation for $C_3$ plants. $X_{ref}$ stands for $g_m$, $A_{m,max}$ or $\Gamma$ at reference temperature of 298K. source: Ronda et al. (2001)

| *Parameter* | *Function of* | $X_{ref}$ | $Q_{10}$ | $T_1(K)$ | $T_2(K)$ |
|---|---|---|---|---|---|
| $f_min[-]$ | | 0.89 | | | |
| $K_x[-]$ | | 0.6 | | | |
| $a_d[Pa^{-1}]$ | | 0.07E-3 | | | |
| $\alpha_0[kg\ J^{-1}]$ | | 0.017E-3 | | | |
| $\Gamma[kg\ m^{-3}]$ | T | 68.5E-6$\rho_a$ | 1.5 | | |
| $g_m[m\ s^{-1}]$ | T | 0.007 | 2.0 | 278 | 301 |
| $A_{m,max}[kg\ m^{-2}\ s^{-1}]$ | T | 0.0022 | 2.0 | 281 | 311 |

$f_{min}$ occurs when the stomata close. The stomata will close when there is very dry air (i.e. very high $VPD$). This happens at $VPD_0$:

$$VPD_0 = \frac{f_{max} - f_{min}}{a_d} \quad , \tag{B12}$$

where $a_d$ is a constant.

## REFERENCES


Bergot, T., J. Escobar, and V. Masson, 2014: Effect of small scale surface heterogeneities and buildings on radiation fog : Large-Eddy Simulation study at Paris-Charles de Gaulle airport. *Q.J.R. Meteorol. Soc.*, n/a–n/a, doi:10.1002/qj.2358.

Brodrick, R., M. Bange, S. Milroy, and G. Hammer, 2013: Physiological determinants of high yielding ultra-narrow row cotton: Canopy development and radiation use efficiency. *Field Crops Res.*, **148**, 86–94, doi:10.1016/j.fcr.2012.05.008.

Chen, F. and J. Dudhia, 2001: Coupling an Advanced Land Surface-Hydrology Model with the Penn State-NCAR MM5 Modeling System. Part I: Model Implementation and Sensitivity. *Mon. Weather Rev.*, **129**, 569–585, doi:10.1175/1520-0493(2001)129⟨0587:CAALSH⟩2.0.CO;2.

Collatz, J., J. Ball, C. Grivet, and J. Berry, 1991: Physiological and environmental regulation of stomatal conductance, photosynthesis and transpiration: a model that includes a laminar boundary layer. *Agric. Forest Met.*, **54**, 107–136, doi:10.1016/0168-1923(91)90002-8.

Collatz, J., J. Ball, C. Grivet, and J. Berry, 1992: Coupled Photosynthesis-Stomatal conductance model for leaves of C4 plants. *Aust. J. Plant Physiol.*, **19**, 519–538, doi:10.1071/PP9920519.

Dengel, S. and J. Grace, 2010: Carbon Dioxide Exchange and canopy conductance of two coniferous forests under various sky conditions. *Oecologia*, **164 (3)**, 797–808, doi:10.1007/s00442-010-1687-0.

Doms, G., et al., 2011: A description of the nonhydrostatic regional COSMO model. Part II: physical parameterization. Tech. rep., COSMO. URL `http://www.cosmo-model.org/content/model/documentation/core/cosmoPhysParamtr.pdf`.

ECMWF, 2012: IFS Documentation Cy38r1. Tech. rep. URL `http://www.ecmwf.int/research/ifsdocs/CY38r1/`, (visited June 2013).

Evers, J., N. Huth, and M. Renton, 2009: Light Extinction in Spring Wheat Canopies in Relation to Crop Configuration and Solar Angle. *Plant Growth Modeling, Simulation, Visualization and Applications (PMA), 2009 Third International Symposium on*, 107–110, doi:10.1109/PMA.2009.20.

Farquhar, G. and T. Sharkey, 1982: Stomatal conductance and photosynthesis. *Ann. Rev. Plant Physiol.*, **33 (1)**, 317–345, doi:10.1146/annurev.pp.33.060182.001533.

Field, C., J. Berry, and H. Mooney, 1982: A portable system for measuring carbon dioxide and water vapour exchange of leaves. *Plant. Cell and Env.*, **5**, 179–186, doi:10.1111/1365-3040.ep11571607.

Foken, T., 2008: The energy balance closure problem: An overview. *Ecol. Applic.*, **18 (6)**, 1351–1367, doi:10.1890/06-0922.1.

Gorton, H., W. Williams, and S. Assmann, 1993: Circadian rhythms in stomatal responsiveness to Red and Blue light. *Plant Phys.*, **103**, 399–406, doi:10.1104/pp.103.2.399.

Gotway, J., et al., 2012: Model Evaluation Tools Version 4.0. Users guide 4.0.1. Tech. rep., Developmental Testbed Center, Boulder, Colorado, USA. URL `http://www.dtcenter.org/met/users/docs/users_guide/MET_Users_Guide_v4.0.1.pdf`, (visited June 2013).

Graf, A., et al., 2010: Boundedness of Turbulent Temperature Probability Distributions, and their Relation to the Vertical Profile in the Convective Boundary Layer. *Bound.-Layer Meteor.*, **134 (3)**, 459–486, doi:10.1007/s10546-009-9444-9.

Graser, E., S. Verma, and N. Rosenberg, 1987: Within-canopy temperature patterns of sorghum at two row spacings. *Agric. Forest Met.*, **41 (3-4)**, 187–205, doi:10.1016/0168-1923(87)90079-7.

Hartogensis, O., 2006: Exploring Scintillometry in the Stable Atmospheric Surface Layer. Ph.D. thesis, Wageningen University, p. 228.

Hartogensis, O., H. De Bruin, and B. Van De Wiel, 2002: Displaced-Beam Small Aperture Scintillometer Test. Part II: Cases-99 Stable Boundary-Layer Experiment. *Bound.-Layer Meteor.*, **105 (1)**, 149–176, doi:10.1023/A:1019620515781.

Hogewoning, S., G. Trouwborst, H. Maljaars, H. Poorter, W. Van Ieperen, and J. Harbinson, 2010: Blue light dose-responses of leaf photosynthesis, morphology, and chemical composition of Cucumis sativus grown under different combinations of red and blue light. *J. Exp. Bot.*, **61 (11)**, 3107–3117, doi:10.1093/jxb/erq132.

Holtslag, A. and M. Ek, 1996: Simulation of surface fluxes and boundary layer development over the pine forest in HAPEX MOBILHY. *J. Appl. Meteor.*, **35 (2)**, 202–213, doi:10.1175/1520-0450(1996)035⟨0202:SOSFAB⟩2.0.CO;2.

Huete, A., K. Didan, T. Miura, E. Rodriguez, X. Gao, and L. Ferreira, 2002: Overview of the radiometric and biophysical performance of the MODIS vegetation indices. *Rem. Sens. Env.*, **83 (1-2)**, 195–213, doi:10.1016/S0034-4257(02)00096-2.

Irmak, S. and D. Mutiibwa, 2010: On the dynamics of canopy resistance: Generalized linear estimation and relationships with primary micrometeorological variables. *Water Res. Research*, **46 (8)**, n/a–n/a, doi:10.1029/2009WR008484.

Jacobs, C., 1994: Direct impact of atmospheric CO2 enrichement on regional transpiration. Ph.D. thesis, Wageningen University, p. 179.

Jacobs, C. M. J., et al., 2007: Variability of annual CO2 exchange from Dutch grasslands. *Biogeosciences*, **4 (5)**, 803–816, doi:10.5194/bg-4-803-2007.

Jacquemin, B. and J. Noilhan, 1990: Sensitivity study and validation of a land-surface parameterization using the HAPEX-MOBILHY data set. *Bound.-Layer Meteor.*, **52 (1-2)**, 93–134, doi:10.1007/BF00123180.

Janssens, I. A., et al., 2001: Productivity overshadows temperature in determining soil and ecosystem respiration across European forests. *Glob. Change Biol.*, **7 (3)**, 269–278, doi:10.1046/j.1365-2486.2001.00412.x.

Jarvis, P., 1976: The Interpretation of the Variations in Leaf Water Potential and stomatal Conductance Found in Canopies in the Field. *Phil. Trans. R. Soc. Lond. B.*, **273 (927)**, 596–610, doi:10.1098/rstb.1976.0035.

Kim, J. and S. Verma, 1991: Modeling canopy stomatal conductance in a temperate grassland ecosystem. *Agric. Forest Met.*, **55**, 149–166, doi:10.1016/0168-1923(91)90028-O.

Lloyd, J. and J. A. Taylor, 1994: On the Temperature Dependence of Soil Respiration. *Func. Ecol.*, **8 (3)**, 315–323, URL `http://www.jstor.org/stable/2389824`.

Manzoni, S., G. Vico, A. Porporato, and G. Katul, 2013: Biological constraints on water transport in the soil-plant-atmosphere system. *Adv. Water Res.*, **5**, 292–304, doi:10.1016/j.advwatres.2012.03.016.

Maronga, B., A. Moene, D. Van Dinther, S. Raasch, F. Bosveld, and B. Gioli, 2013: Derivation of Structure Parameters of Temperature and Humidity in the Convective Boundary Layer from Large-Eddy Simulations and Implications for the Interpretation of Scintillometer Observations. *Bound.-Layer Meteor.*, **148 (1)**, 1–30, doi:10.1007/s10546-013-9801-6.

Moene, A. and J. Van Dam, 2014: *Atmosphere-Vegetation-Soil Interactions*, chap. Vegetation: Transport processes inside and outside of plants., 184–231. Cambridge University Press.

Moriasi, D., J. Arnold, M. Van Liew, R. Bingner, R. Harmel, and T. Veith, 2007: Model evaluation guidelines for systematic Quantification of accuracy in watershed simulations. *Trans. ASABE*, **50 (3)**, 885–900, doi:10.13031/2013.23153.

Mott, K. A., 1990: Sensing of atmospheric CO2 by plants. *Plant, Cell and Env.*, **13 (7)**, 731–737, doi:10.1111/j.1365-3040.1990.tb01087.x.

Nash, J. and J. Sutcliffe, 1970: River flow forecasting through conceptual models part I - a discussion of principles. *J. Hydr.*, **10 (3)**, 282–290, doi:10.1016/0022-1694(70)90255-6.

Op de Beeck, M., M. De Bock, M. Vandermeiren, L. De Temmerman, and R. Ceulemans, 2010: comparison of two stomatal conductance models for ozone flux modeling using data from two Brassica species. *Environ. Poll*, **185**, 3251–3260, doi:10.1016/j.envpol.2010.07.026.

Ott, R. and M. Longnecker, 2010: *An introduction to Statistical methods and data analysis.*, chap. Linear regression and correlation. 6th ed., Brooks/Cole, Cengage Learning.

Pitman, A. J., 2003: The evolution of, and revolution in, land surface schemes designed for climate models. *Int. J. Climatol.*, **23 (5)**, 479–510, doi:10.1002/joc.893.

Raghavendra, A., V. Gonugunta, A. Christmann, and E. Grill, 2010: ABA perception and signalling. *Trends in Plant Sci.*, **15 (7)**, 395–401, doi:10.1016/j.tplants.2010.04.006.

Rambal, S., J.-M. Ourcival, R. Joffre, F. Mouillot, Y. Nouvellon, M. Reichstein, and A. Rocheteau, 2003: Drought controls over conductance and assimilation of a Mediterranean evergreen ecosystem: scaling from leaf to canopy. *Glob. Change Biol.*, **9 (12)**, 1813–1824, doi:10.1111/j.1365-2486.2003.00687.x.

Reichstein, M., et al., 2005: On the separation of net ecosystem exchange into assimilation and ecosystem respiration: review and improved algorithm. *Glob. Change Biol.*, **11 (9)**, 1424–1439, doi:10.1111/j.1365-2486.2005.001002.x.

Ronda, R., H. De Bruin, and A. Holtslag, 2001: Representation of the canopy conductance in modelling the surface energy budget for low vegetation. *J. Appl. Meteor.*, **40**, 1431–1444, doi:10.1175/1520-0450(2001)040⟨1431:ROTCCI⟩2.0.CO;2.

Smith, E., N. Tolbert, and H. Ku, 1976: Variables affecting CO2 compensation point. *Plant Phys.*, **58 (2)**, 143–146, doi:?10.?1104/?pp.?58.?2.?143.

Stewart, J., 1988: Modeling surface conductance of pine forest. *Agric. Forest Met.*, **43**, 19–35, doi:10.1016/0168-1923(88)90003-2.

Tatarskii, V., 1961: *Wave propagation in a turbulent medium*. McGraw-Hill Book Company Inc., New York, 285 pp.

Thiermann, V. and H. Grassl, 1992: The measurement of turbulent surface-layer fluxes by use of bichromatic scintillation. *Bound.-Layer Meteor.*, **58 (4)**, 367–389, doi:10.1007/BF00120238.

Unden, P., et al., 2002: HIRLAM 5.0 Scientific Documentation. URL `http://citeseerx.ist.psu.edu/viewdoc/summary?doi=10.1.1.6.3794`, URL `http://citeseerx.ist.psu.edu/viewdoc/summary?doi=10.1.1.6.3794`.

Urban, O., et al., 2012: Impact of clear and cloudy sky conditions on the vertical distribution of photosynthetic CO2 uptake within a spruce canopy. *Func. Ecol.*, **26 (1)**, 46–55, doi:10.1111/j.1365-2435.2011.01934.x.

van Heerwaarden, C., J. Vilà-Guerau de Arellano, A. Moene, and A. Holtslag, 2009: Interactions between dry-air entrainment, surface evaporation and convective boundary-layer development. *Q.J.R. Meteorol. Soc.*, **135 (642)**, 1277–1291, doi:10.1002/qj.431.

Van Kesteren, B., O. Hartogensis, D. Van Dinther, A. Moene, and H. De Bruin, 2013a: Measuring H2O and CO2 fluxes at field scales with scintillometry: Part I - Introduction and validation of four methods. *Agric. Forest Met.*, **178-179**, 75–87, doi:10.1016/j.agrformet.2012.09.013.

Van Kesteren, B., O. Hartogensis, D. Van Dinther, A. Moene, and H. De Bruin, 2013b: Measuring H2O and CO2 fluxes at field scales with scintillometry: Part II-application and validation of 1-min flux estimates. *Agric. Forest Met.*, **178-179**, 88–105, doi:10.1016/j.agrformet.2013.01.010.

Vico, G., S. Manzoni, S. Palmroth, and G. Katul, 2011: Effects of stomatal delays on the economics of leaf gas exchange under intermittent light regimes. *New Phytol.*, **192 (3)**, 640–652, doi:10.1111/j.1469-8137.2011.03847.x.

Vilà-Guerau de Arellano, J., H. Ouwersloot, D. Baldocchi, and C. Jacobs, 2014: Shallow cumulus rooted in photosynthesis. *Geophys. Res. Lett.*, n/a–n/a, doi:10.1002/2014GL059279.

Vilà-Guerau de Arellano, J., C. C. Van Heerwaarden, and J. Lelieveld, 2012: Modelled suppression of boundary-layer clouds by plants in a CO2-rich atmosphere. *Nat. Geosc.*, **5**, 701–704, doi:10.1038/ngeo1554.

Waggoner, P. and W. Reifsnyder, 1968: Simulation of the Temperature, Humidity and Evaporation Profiles in a Leaf Canopy. *J. Appl. Meteor.*, **7**, 400–409, doi:10.1175/1520-0450(1968)007⟨0400:SOTTHA⟩2.0.CO;2.

Wong, S., 1979: Stomatal behaviour in relation to photosynthesis. Ph.D. thesis, Australian National University, p. 191.

Woods, D. and N. Turner, 1971: stomatal response to changing light by four tree species of varying shade tolerance. *New Phytol.*, **70 (1)**, 77–84, doi:10.1111/j.1469-8137.1971.tb02512.x.

Zhang, H. and P. Nobel, 1996: Dependency of ci/ca and Leaf transpiration Efficiency on the vapour pressure deficit. *Aust. J. Plant Physiol.*, **23 (5)**, 561–568, doi:10.1071/PP9960561.